

Freezing desalination of sea water in a static layer crystallizer

Anouar Rich^{a,b,c}, Youssef Mandri^{a,b,c}, Nourimane Bendaoud^{a,b,c}, Denis Mangin^{a*},
Souad Abderafi^b, Christine Bebon^a, Naoual Semlali^b, Jean-Paul Klein^a, Tijani Bounahmidi^b,
Ahmed Bouhaouss^c, Stephane Veessler^d

^aLaboratoire d'Automatique et de Génie des Procédés, UMR CNRS 5007, Université Lyon 1, Université de Lyon, CPE Lyon, 43 bd du 11 novembre 1918, F-69622 Villeurbanne, France

Tel. +33 (4) 72 43 18 51; Fax +33 (4) 72 43 16 82; email: mangin@lagep.univ-lyon1.fr

^bLaboratoire d'Analyse et de Synthèse des Procédés Industriels, Ecole Mohammadia d'Ingénieurs (EMI), Université Mohammed V-Agdal, Rabat, Maroc

^cLaboratoire de Chimie Physique Générale I des Matériaux, Nanomatériaux et Environnement, Faculté des Sciences, Université Mohammed V-Agdal, Rabat, Maroc

^dCentre Interdisciplinaire de Nanoscience de Marseille, CINAM-CNRS, Campus de Luminy, Case 913, 13288 Marseille, France

Received 3 May 2009; accepted 3 November 2009

ABSTRACT

This work aims in developing a static layer crystallizer for freezing desalination of sea water. The experiments were performed with a simple system of H₂O–NaCl and with samples of sea water from Rabat. The pilot crystallizer consists in a tube cooled by means of a thermostatic bath. The tube is immersed in a cylindrical double jacketed tank cooled by means of a second thermostatic bath. The brine is poured into the tank and the crystallization takes place on the external surface of the tube. The global process is divided into 4 steps: (i) crystallization of the ice layer by controlling the cooling rate in the tube (ii) draining off the concentrated brine (iii) purification of the layer by sweating and (iv) melting of the ice to recover the fresh water. A parametric study of the effect of the operating parameters has allowed us to quantify the role of the different key parameters of the crystallization step. Within the studied domain, the purity of the crystalline layer was mainly affected by the initial salinity of the brine. The growth rate of the layer, controlled by the cooling rate in the tube, had also a significant effect. Experiments performed with Rabat sea water showed that a fresh water of salinity close to the drinking water standards could be obtained in one stage within 31 h. Desalination operated in two consecutive stages (10 h + 11 h) gave salinity below the standards with a comfortable safety margin. If sufficiently severe operating conditions are applied, sweating is able to purify the interior of the ice layer and to reach the drinking water standards, provided the impurity concentration of the ice produced in the crystallization step is low enough. The mass loss induced by sweating is also high when the impurity concentration is high. These first results are promising and show the feasibility of the process which still requires to be optimized.

Keywords: Freezing desalination; Melt crystallization; Sea water; Crystal layer growth; Sweating

1. Introduction

To satisfy the needs of fresh water which are increasingly important, much research has been

*Corresponding author

conducted to find effective methods of desalination that can remove salt from sea water. Desalination methods used are distillation (Multi-stage flash distillation; Multiple-effect distillation; and Vapour compression distillation) and reverse osmosis. However several authors have proposed the method of freezing as an alternative to the distillation and reverse osmosis for desalination [1–5], treatment of wastewater [5–8], or the concentration of food solutions [9–12]. The process of desalination by freezing could be advantageous by comparison with reverse osmosis and distillation. The energy cost of desalination by freezing could be similar to that of reverse osmosis, but the investment and operation costs might be lower since the membranes of reverse osmosis are sensitive to the problem of fouling and require a thorough pretreatment of the seawater. The freeze process should also be less affected by corrosion and scaling than distillation, thanks to the low levels of the working temperatures. Finally, the energy consumption could be lower than it is in distillation, because the heat of fusion of ice is seven times lower than the heat of vaporization of water.

There are two possible methods in freezing: direct and indirect freezing. The principle of direct freezing is the formation of ice crystals by contact of a refrigerant with the seawater. In some cases, the refrigerant can be the seawater itself: heat is removed from the brine by flash vaporization of a water fraction at low pressure. This process is called the vacuum freezing vapour compression (VFVC). The second alternative for direct freezing is the secondary refrigerant freeze (SRF) process. The cooling is obtained by the expansion of a compressed and cold gas directly injected in the brine [13].

In the indirect process, freezing is conducted by circulating the refrigerant through a heat exchanger and the heat is removed by conduction.

Several pilot plants using freezing desalination have been developed during the last years, but the technology has never been used commercially to produce drinking water [14]. The pilot plant of Wrightsville beach in North Carolina (USA) and the pilot plant of Eilat (Israel) used both the VFVC technology; the unit built in Florida (USA) was based on the SFR process [15]; the pilot plant of Yanbu (Saudi Arabia) used the technique of indirect freezing [16].

This work deals with indirect freezing desalination. The apparatus is a static layer crystallizer that permits the crystallization, the sweating and the melting operations in the same tank. Most of the experiments were carried out with an initial solution formed of water and NaCl. The purity of the ice obtained after the crystallization step was studied as a function of the crystal growth rate and the initial salinity of the brine.

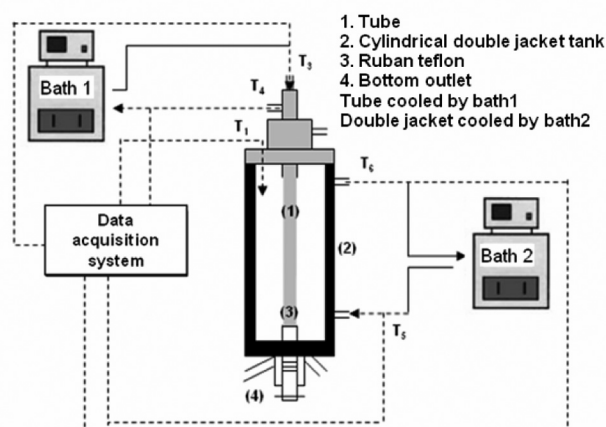


Fig. 1. Experimental apparatus of the freeze desalination process in static.

Preliminary results on the efficiency of the following purification step by sweating were also obtained.

2. Material and method

2.1. Experimental setup and procedure

Fig. 1 represents the experimental setup. It was composed of a stainless steel tube (316 L) immersed inside a cylindrical double jacketed tank. Two thermostatic baths were used to adjust the temperature of the coolant fluids circulating in the tube and in the double jacketed tank, respectively. The different temperatures were measured and recorded continuously using a data acquisition system (Compact Field-Point with software LabVIEW of National Instrument). The Pt100 probes used were calibrated with a reference at 0 °C (water + ice at the atmospheric pressure), on one hand, and with a calibrated probe, on the other hand. After calibration, a precision of 0.05 °C was obtained in the temperature domain [–10 °C; 5 °C].

The solution (seawater or water/NaCl) was introduced into the glass tank. Freezing was carried out on the external surface of the tube. At the bottom, the tube was covered with Teflon to avoid crystallization in this zone. The jacketed glass tank allowed visual observation of the ice layer formation.

The freezing step, i.e. the crystallization step, was conducted by maintaining a constant temperature in the double jacket of the glass tank and by operating a linear cooling ramp in the tube. It was necessary to initialize the crystallization process. In fact, the metastable zone of the heterogeneous primary nucleation of the ice on the tube surface is large. Preliminary tests showed, for example, that with an aqueous solution

Table 1
Parametric study of the crystallization step (notations explained in the text)

Run	C (g/kg)	T_I (°C)	T_F (°C)	Δt (h)	T_{DJ} (°C)	m_{ice}^0 (g)	C_{ice}^0 (g/kg)	C_{ice}^1 (g/kg)	m_{WA} (g)	C_{WA} (g/kg)	m_S (g)	C_S (g/kg)
1	17.15 ($T_{eq} = -1$ °C)	-1.20	-1.6	5	1	31.35	0.92	–	–	–	269.85	18.93
2		-1.20		7		30.40	0.64	–	–	–	269.76	19.03
3		-1.30		14		32.47	0.40	–	–	–	267.09	19.29
4		-1.30		24		34.7	0.34	–	–	–	265.55	19.19
11	25 ($T_{eq} = -1.46$ °C)	-1.75	-2.2	5	0.5	33.18	2.55	1.82	0.86	29.88	267.50	27.60
12		-1.75		7		36.56	1.45	1.08	0.53	26.77	262.49	28.44
13		-1.75		14		36.05	0.87	0.49	0.4	34.46	264.20	28.30
14		-1.75		24		36.62	0.69	0.46	0.29	29.744	261.74	28.41
19	35 ($T_{eq} = -2$ °C)	-2.30	-2.9	5	0	29.48	7.04	5.79	1.05	40.85	270.05	38.03
20		-2.30		7		28.81	4.23	2.99	1.45	27.61	272.20	38.23
21		-2.30		14		31.84	2.05	1.76	0.23	41.25	268.05	38.83
22		-2.30		24		34.46	0.86	0.58	0.30	32.07	264.74	39.50
23	52.5 ($T_{eq} = -3.06$ °C)	-3.35	-4.2	5	-1.1	29.29	18.27	15.49	1.86	59.29	270.36	56.31
24		-3.35		7		32.76	9.84	7.97	1.16	60.69	267.45	57.46
25		-3.35		14		30.84	5.71	4.82	0.49	61.03	266.9	58.98
26		-3.35		24		31.63	3.68	2.99	0.38	60.40	268.26	58.21
31	65 ($T_{eq} = -3.8$ °C)	-4.10	-5.2	5	-1.8	31.40	26.14	21.54	2.77	73.64	267.45	69.56
32		-4.10		7		32.24	23.23	19.72	2.04	75.13	265.91	70.14
33		-4.10		14		35.04	10.54	8.92	0.89	72.62	264.13	72.13
34		-4.10		24		34.33	9.26	8.57	0.33	80.10	264.75	73.28

containing 35 g/kg of NaCl and for an undercooling of 3.5 °C below the equilibrium temperature, the retention time required to start the nucleation on the tube surface was longer than 20 min. In practice, the crystallization was initialized as follows: the tube was first cooled to -6 °C and plunged in distilled water in order to form a thin ice layer on the surface of the tube (mass ranging between 1 and 2 g); the temperature in the tube was then quickly raised to the initial value of the crystallization step; the tube covered by the thin ice layer was finally introduced in the glass tank filled with 300 g of saline solution and the cooling rate was applied in the tube. At the end, the chosen final temperature was kept constant for 1 h. The brine was withdrawn through the bottom outlet. In the parametric study of the crystallization step, the ice surface was washed by leaving the ice layer in the air at ambient temperature for 10 min. The ice surface slightly melted and the solution was recovered. Finally, the tube temperature was increased in order to completely melt the ice layer. Sweating was also processed in several experiments. It consists in a controlled heating of the crystalline layer in order to melt the crystal sections with higher impurity concentration. Sweating is then able to purify the interior of the ice layer by draining out included impurities. Two methods were applied. In the experiments performed with sea water, the temperature was linearly increased from the final temperature of the crystallization step to the chosen

final sweating temperature during 1 h. In the experiments performed for the sweating study, the sweating temperature was set to the chosen value immediately after the crystallization step and kept constant during the whole sweating step. Systematically, the different solutions collected (brine, drained out liquid by washing or sweating and melted ice) were weighted and their salinities were measured.

2.2. Solution analysis

Two types of solutions were used: Rabat sea water and synthetic water/NaCl solutions. The sea water and the solutions produced in the sea water desalination experiments were analyzed by Inductively Coupled Plasma-Atomic Emission Spectroscopy (ICP-AES). This analytical technique is able to measure the content of almost all the elements present in aqueous solutions. The salinity of the water/NaCl solutions was measured by weighting the dry extract of a solution sample of known mass, dried in an oven at 90 °C during 12 h.

3. Parametric study of the crystallization step

All the experiments were performed with synthetic water/NaCl solutions. The operating conditions tested are given in Table 1. The salinity of the initial solution C is indicated in the second column. The ice/solution

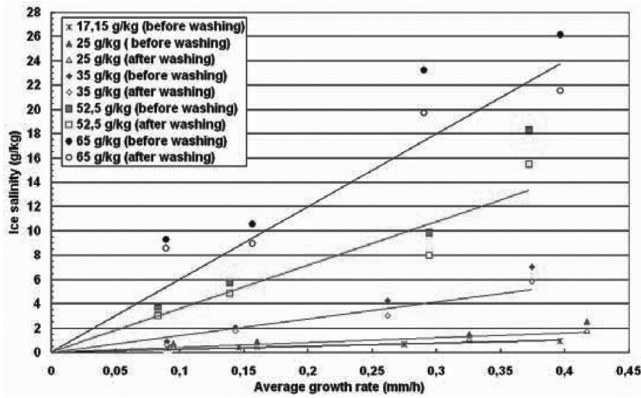


Fig. 2. Ice salinity versus average growth rate.

equilibrium temperature calculated with Pitzer model [17–22] is also given between brackets in this column. The operating parameters of the cooling rate of the crystallization step were the initial temperature in bath n°1, T_I , the final temperature in bath n°1, T_F and the cooling time, Δt . T_I was determined experimentally for each initial salinity. It was the optimal temperature which allowed regular growth of the ice layer from the beginning of the crystallization step. Higher values induced slight initial dissolution of the seed ice lining. Lower values induced initial fast growth. T_I is slightly lower than the equilibrium temperature because of the heat transfer resistance. The temperature in bath n°2, connected to the double jacket of the glass tank was fixed at T_{DJ} during the whole crystallization step. T_{DJ} was chosen in order to have similar temperature differences between the tube and the double jacket in all the experiments (about 2.2 °C at the beginning of the cooling rate). m_{ice} is the mass of ice produced before washing. It is the total mass, corrected by the mass of the seed ice lining formed in distilled water to initialize the crystallization. m_{ice}^0 is directly linked to the final temperature T_F . However, the masses obtained were generally smaller in the experiments performed at the shortest cooling time. This could suggest that the equilibrium is not reached at the end of the shortest experiments, even after the final stabilization step of 1 h. C_{ice}^0 and C_{ice}^1 are the salinities of the ice, before and after washing, respectively. m_{WA} is the mass of solution collected during washing and C_{WA} is its salinity. Finally, m_S is the mass of brine and C_S is its salinity. The global mass balances and the salt mass balances give a relative error of less than 1% with all experiments.

Fig. 2 shows the evolution of the ice salinity as a function of the average growth rate for different initial solution salinities. The average growth rate is calculated with m_{ice}^0 and Δt , considering the cylindrical geometry. For each growth rate, the two points

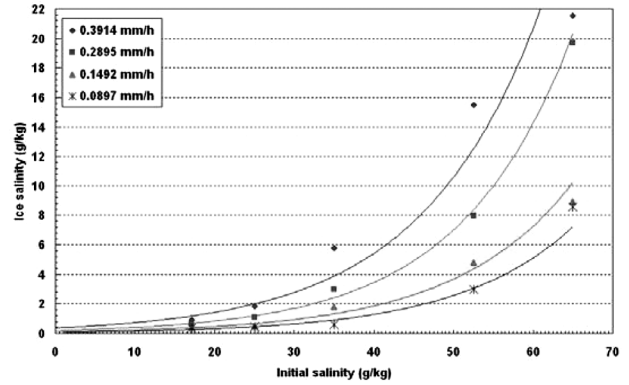


Fig. 3. Ice salinity versus initial solution concentration for different ice growth rates.

correspond to the ice salinity obtained before and after washing, respectively. Fig. 2 clearly shows that the ice salinity increases with the growth rate. The increase is more or less linear. The different lines drawn correspond to the salinities reached after washing. The washing step induced a significant decrease of the ice salinity. This could be due to the low mass of ice. Indeed, the amount of brine that still wets the ice surface after the brine has been drained off might be not negligible, compared with the ice mass. The ice salinity strongly increases with the initial solution salinity (Fig. 3). The ice impurities are due to inclusion of drops or pockets of brine. For a given growth rate, one could expect that the number of inclusion is the same, whatever the concentration of the mother solution. Thus, the strong increase of ice salinity observed in Fig. 3 might suggest that the solution concentration gradient at the ice/brine interface during the growth step would be higher with higher brine concentration. Fig. 4 gives two typical temperature profiles for mother solution initially at 25 g/kg and 65 g/kg, respectively. These temperatures were measured in the solution with the

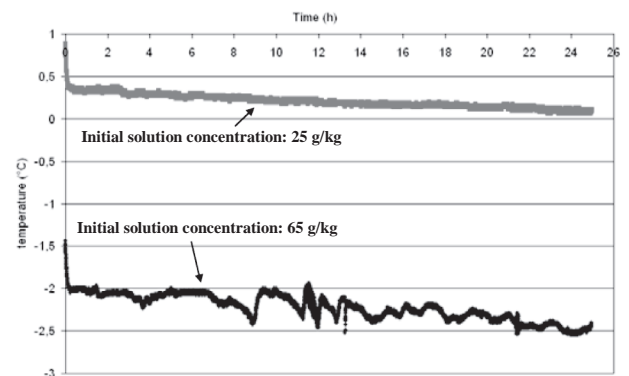


Fig. 4. Temperature profiles measured in solution (runs n° 14 and 34).

Table 2
Desalination of sea water in one and two stages

Run	m_i (g)	Solution	T_I (°C)	T_F (°C)	Δt (h)	T_{SW} (°C)	Δt_{SW} (min)	C_{ice} (g/kg)	m_{ice} (g)	C_s (g/kg)	m_s (g)	C_{SW} (g/kg)	m_{SW} (g)
43	300	Sea water	-2	-5.7	30	-0.5	60	0.85	113.8	75.01	186.47	49.1	2.86
44	300	Sea water	-2	-5.7	7	-0.5	60	6.52	97.1	67.6	192.01	46	13.04
45	310	Sea water	-2	-5.7	9	-0.5	35	6.82	107.42	64.38	196.42	50.78	6.82
46			-2	-5.7	9	-0.5		7.50	104.60	64.23	193.24	43.77	12.09
47			-2	-5.7	9	-0.5		6.80	100.45	63.59	197.76	43.65	10.83
48	298.34	7.27 g/kg (melted ice)	-0.5	-2	10	-0.3	35	0.16	114.61	11.7	182.57	11.2	1.64
49	300	7.01 g/kg (melted ice)	-0.5	-2	10	-0.3	35	0.29	120.09	11.63	180.03	0	0

probe quoted T_I , in Fig. 1. The curve relative to the higher brine concentration shows fluctuations. This might be due to more significant convection current, induced by higher concentration gradients. Closer observations are necessary to confirm this hypothesis.

As concern the desalination process, the important influence of the brine concentration on the ice salinity could suggest to stop the crystallization process before the brine concentration increases too much. However, this would be more energy consuming since all the solution has to be cooled. An optimum has to be found. It can also be noticed that salinities of about 0.5 g/kg or less than this value were reached in the slowest experiments of initial salinity of less or equal to 35 g/kg. Desalinated water of maximum salinity equal to 0.5 g/kg is generally considered to satisfy the drinking water standards. For initial salinity of 35 g/kg, corresponding to sea water salinity, only the experiment performed at the slowest growth rate of 0.09 mm/h gave almost drinking water. For lower initial salinities, higher growth rate could be used to produce drinking water. This shows that the standards of drinking water might be reached in one stage, provided the chosen growth rate is very low. This also suggests that the standards should be more easily satisfied if the desalination process is operated in two stages, which would be more energy consuming. However, note that these results were obtained with a simple surface washing of the ice layer. As shown in part 5, sweating is able to strongly improve the ice purity.

4. Freezing desalination of Rabat sea water

The experiments were carried out with Rabat sea water. Table 2 gives the operating conditions and the experimental results. m_i is the initial mass of solution; T_I , T_F and Δt are the initial temperature, the final temperature and the duration of the crystallization step, respectively; T_{SW} and Δt_{SW} are the final temperature

and the duration of the sweating step; C_{ice} and m_{ice} are the salinity and the mass of the ice after sweating; C_s and m_s are the salinity and the mass of the brine; C_{SW} and m_{SW} are the salinity and the mass of the solution collected during the sweating step. All the experiments were done with a double jacket temperature T_{DJ} equal to 3 °C.

Experiments 43 and 44 differ by the applied growth rates. The salinity obtained in the fasted experiment is much higher, which confirms the great importance of the growth rate on the ice purity. Besides, the short sweating step does not seem to correspond to a simple surface washing. It is probably able to also purify the interior of the ice layer, at least partly, since the mass of recovered solution is much higher in the case of the most impure ice layer. In 30 h (run 43), the final salinity is close to the standards of drinking water after the sweating step. Again, we see that slow growth rate seems to be able to satisfy the standards in one stage operation. The average growth rate in run 43 was about 0.2 mm/h. Calculation of the ice salinity before sweating gives about 2.03 g/kg. If we compare this value with the results of the parametric study recorded in part 3, the salinity obtained is slightly lower (2.03 g/kg here against 3 g/kg in part 3), although the ice mass and the final brine salinity are both higher. A migration of the impurities included in the ice layer might have occurred in experiment 43. This migration of liquid inclusions is induced by the temperature gradient and allows purification of the ice layer during crystallization. This phenomenon might have been more important in run 43, since the temperature gradient was higher and the duration of the experiment was longer.

Runs 45 to 49 deal with Rabat sea water desalination operated in two stages. Runs 45 to 47 correspond to the first stage. The 3 runs are reproducible and the results are consistent with experiment 44. The 312.45 g of ice formed with these 3 runs give a solution of average salinity equal to 7.27 g/kg. Run 48, filled with this

Table 3
Concentrations of the principal elements measured by ICP-AES

Species	Rabat seawater (mg/l)	run 49, Initial solution (mg/l)	run 49, ice (mg/l)	European standards of drinking water (mg/l)
Cl	25703.51	2895.80	152.27	250
Na	10018.40	2091.18	85.50	200
S	1016.59	200.32	10.713	250
Mg	1287.33	282.68	17.23	80
Ca	421.80	109.84	4.24	100
K	630.05	69.89	2.96	12
Sr	5.485	1.170	0.055	–

solution, corresponds to the second stage. Run 49 repeats experiment 48. It was filled with a solution produced with another series of three experiments. Comparison between runs 48 and 49 shows a good reproducibility. The second stage gives a very pure ice, of salinity less than 0.3 g/kg. The two stages allow production of drinking water with a good safety margin. Table 3 compares the concentrations of the principal elements analysed by ICP-AES with the standards. Figs. 5 and 6 show the visual aspect of the ice formed after the first and the second stage, respectively. Lost of inclusions can be observed in the ice of the first stage. The ice of the second stage is perfectly transparent.

5. Sweating study

For this study, each experiment was done with an ice layer of about 100 g, corresponding to an ice thickness of about 5.4 mm. The ice layer was produced under controlled operating conditions in order to obtain the wondered salinity. Three ice salinities were tested.

Fig. 7 compares the concentration of the ice after and before sweating for different sweating temperatures and sweating times. For a given sweating time of 2 h, an increase of the sweating temperature from $-0.8\text{ }^{\circ}\text{C}$ to $0\text{ }^{\circ}\text{C}$ improves the purity by a salinity drop of about 2 g/kg. For a given temperature of $0\text{ }^{\circ}\text{C}$, the increase of the sweating time improves the purity of the two tested ices, the drop being more important with the ice of higher initial concentration. With $T_{\text{SW}} = 0\text{ }^{\circ}\text{C}$, $\Delta t_{\text{SW}} = 8\text{ h}$ and for initial concentration of 14.68 g/kg, sweating was impossible during 8 h, because the ice became detached of the tube. For the other initial concentrations, the ice salinity after sweating was systematically lower than the standards of drinking water. Globally, sweating allows important purification. For given temperature and time, the ice purity after sweating is better when the initial ice

concentration is lower. However, a limitation is observed, when extreme sweating conditions (i.e. $T_{\text{SW}} = 0\text{ }^{\circ}\text{C}$ and $\Delta t_{\text{SW}} = 8\text{ h}$) are applied.

The effect of ice initial concentration on the mass loss of the ice for different sweating temperatures and sweating times is shown in Fig. 8. Obviously, the mass loss is directly linked to the purification rate observed in Fig. 7. This mass loss is energy consuming. From these experiments, it appears that, with severe operating conditions, sweating is able to purify the interior of the ice layer and to reach the standards of drinking



Fig. 5. Image of the ice of salinity 6.82 g/kg recovered in the 1st stage of sea water desalination (run 45).



Fig. 6. Image of the ice of salinity 0.16 g/kg recovered in the 2nd stage of sea water desalination (run 48).

water, but the mass loss is high when the initial layer impurity concentration is high.

6. Conclusion

In the present study, the different parameters influencing the process of seawater freezing are tested using a static layer crystallizer. In the crystallization step, the purity of the ice layer is strongly dependant on the growth rate and on the solution concentration. The ice

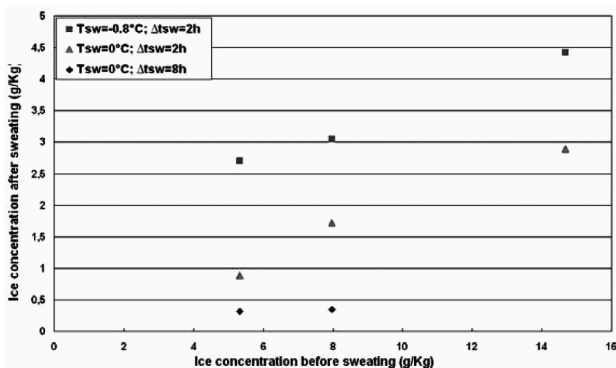


Fig. 7. Effect of sweating parameters on ice purity.

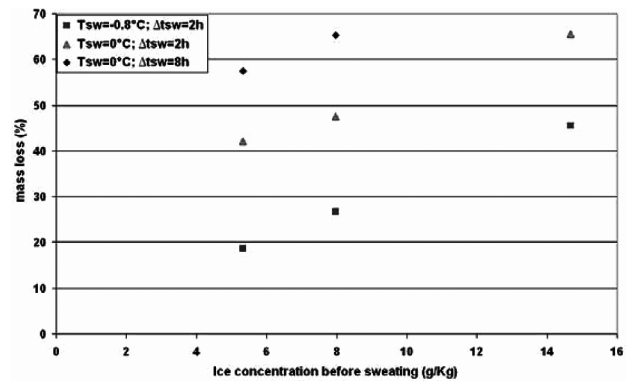


Fig. 8. Effect of sweating parameters on mass loss.

is contaminated by liquid inclusions containing the impurities. Lower growth rates are able to significantly reduce these inclusions. An increase of the brine salinity leads to strong decrease of the ice purity. The sweating step is able to efficiently complete the purification but the mass loss can be important. The global process of desalination, involving both the crystallization and the sweating steps has to be optimized in order to produce drinking water with high recovery rate. The results presented in this work show the feasibility of an indirect freeze desalination process and can be used for its optimization.

Acknowledgements

This study was supported by the French-Moroccan Committee (Comité Mixte Interuniversitaire Franco-Marocain), Hubert Curien/Volubilis program (Action Intégrée n° MA/06/150); the Committee is gratefully acknowledged.

References

- [1] H.M. Curran, Water desalination by indirect freezing, *Desalination*, 7(3) (1970) 273-284.
- [2] J. Fournier, J.L. Grange and S. Vergara, Water desalination by natural freezing, *Desalination*, 15(2) (1974) 167-175.
- [3] D.W. Johnson, J.L. Lott and C.M. Sliepcevich, The exchange crystallization freeze desalination process, *Desalination*, 18(3) (1976) 231-240.
- [4] E. Wallace Johnson, Indirect freezing, *Desalination*, 31(1-3) (1979) 417-425.
- [5] A. Rodriguez Garcia, Ph. D. thesis, Etude de la congélation comme technique de traitement des eaux: applications spécifiques. Institut National des Sciences appliquées de Toulouse (2004), France.
- [6] Y. Shirai, M. Wakisaka, O. Miyawaki and S. Sakashita, Conditions of producing an ice layer with high purity for freeze wastewater treatment, *J. Food Eng.*, 38(3) (1998) 297-308.
- [7] M. Rodriguez, S. Luque, J.R. Alvarez and J. Coca, A comparative study of reverse osmosis and freeze concentration for the removal of valeric acid from wastewaters, *Desalination*, 127(1), (2000) 1-11.

- [8] M. Wakisaka, Y. Shirai and S. Sakashita, Ice crystallization in a pilot-scale freeze wastewater treatment system, *Chem. Eng. Process.*, 40(3) (2001) 201-208.
- [9] R.W. Hartel and L.A. Espinel, Freeze concentration of skim milk, *J. Food Eng.*, 20 (1993) 101-120.
- [10] Z. Zhang and R. W. Hartel, A multilayer freezer for freeze concentration of liquid milk, *J. Food Eng.*, 29(1) (1996) 23-38.
- [11] P. Chen, X. D. Chen and K. W. Free, An experimental study on the spatial uniformity of solute inclusion in ice formed from falling flows on a sub-cooled surface, *J. Food Eng.*, 39, (1999) 101-105.
- [12] O. Miyawaki, L. Liu, Y. Shirai, S. Sakashita and K. Kagitani, Tubular ice system for scale-up of progressive freeze-concentration, *J. Food Eng.*, 69(1) (2005) 107-113.
- [13] R.A. McCormack and R.K. Andersen, Clathrate Desalination Plant Preliminary Research Study, U.S. Bureau of Reclamation Water Treatment Technology Program Report N° 5, June, (1995).
- [14] D. Akili Khawajia, K. Ibrahim Kutubkhanaha and Jong-Mihn Wieb, Advances in seawater desalination technologies, *Desalination*, 221 (2008) 47-69.
- [15] J.J. McKetta Jr, J.J. McKetta and W.A. Cunningham, 1982, *Encyclopedia of chemical processing and design*, ISBN 082472464X, 9780824724641.
- [16] SOLARS, Yanbu Freezing Plant Weekly Reports, KACST, Saudi Arabia 1985-1986.
- [17] R. J. Spencer, N. Møller and J.H. Weare, The prediction of mineral solubilities in natural waters: A chemical equilibrium model for the Na-K-Ca-Mg-Cl-SO₄-H₂O system at temperatures below 25 °C, *Geochim. Cosmochim. Acta*, 54, (1990) 575-590.
- [18] G.M. Marion, A theoretical evaluation of mineral stability in Don Juan Pond, Wright Valley, Victoria Land, Antarct. Sci., 9 (1997) 92-97.
- [19] M.V. Mironenko, S.A. Grant, G.M. Marion and R.E. Farren, FREZCHEM2: a chemical-thermodynamic model for aqueous solutions at subzero temperatures, CRREL Rep. 97-5, USA Cold Regions Research and Engineering Laboratory, Hanover, NH (1997).
- [20] M. Marion Giles, R. Farren and A.J. Komrowski, Alternative pathways for seawater freezing, *Cold Regions Sci. Tech.*, 9 (1999) 259-266.
- [21] M. Marion Giles and R.E. Farren, Mineral solubilities in the Na-K-Mg-Ca-Cl-SO₄-H₂O system: A re-evaluation of the sulfate chemistry in the Spencer-Møller-Weare model. *Geochim. Cosmo-chim. Acta* 63 (1999) 1305-1318.
- [22] R. Feistel and M. Marion Giles, A Gibbs-Pitzer function for high-salinity seawater thermodynamics, *Prog. Oceanogr.*, 74(4) September (2007) 515-539.